Research in Astronomy and Astrophysics, 25:015007 (17pp), 2025 January
© 2025. National Astronomical Observatories, CAS and IOP Publishing Ltd. All rights, including for text and data mining, AI training, and similar technologies, are reserved. Printed in China.
https://doi.org/10.1088/1674-4527/ad995e
CSTR: 32081.14.RAA.ad995e

# The Impact of Different Effective Models for Star Formation on the Properties of Simulated Milky Way-sized Galaxies

Yiheng Wu[1,2,3] and Volker Springel[3]
[1] Shanghai Astronomical Observatory, Chinese Academy of Sciences, Shanghai 200030, China; wuyiheng@shao.ac.cn
[2] University of Chinese Academy of Sciences, Beijing 100049, China
[3] Max-Planck-Institut für Astrophysik, Karl-Schwarzschild-Straße 1, 85740 Garching, Germany
*Received 2024 November 09; revised 2024 November 15; accepted 2024 November 20; published 2025 January 2*

## Abstract

Hydrodynamical cosmological simulations of galaxy formation such as IllustrisTNG or Auriga have shown considerable success in approximately matching many galaxy properties, but their treatment of the star-forming interstellar medium (ISM) has relied on heuristic sub-grid models. However, recent high-resolution simulations of the ISM that directly resolve the regulation of star formation suggest different mean relations for the dependences of pressure and star formation rate on the average gas density. In this study, we adopt such a modern, physically grounded parameterization inspired by the TIGRESS small-scale simulations. We dub this model TEQS and use it for a detailed comparative analysis of the formation and evolution of a Milky Way-sized galaxy when compared with the widely used TNG model. By employing high-resolution simulations in tall box setups, we first investigate the structural differences expected for these two models when applied to different self-gravitating gas surface densities. Our results indicate that TEQS produces considerably thinner gaseous layers and can be expected to form stellar distributions with smaller scale-height than TNG, especially at higher surface density. To test whether this induces systematic structural differences in cosmological galaxy formation simulations, we carry out zoom-in simulations of 12 galaxies taken from the set of Milky Way-sized galaxies that have been studied in the Auriga project. Comparing results for these galaxies shows that disk galaxies formed with the TEQS model have on average very similar stellar mass but are more concentrated in their central regions and exhibit smaller stellar radii compared to those formed with the TNG model. The differences in the scale-heights of the formed stellar disks are only marginal, however, suggesting that other factors for setting the thickness of the disk are more important than the applied ISM equation-of-state model. Overall, the predicted galaxy structure is quite similar for TNG and TEQS despite significant differences in the employed star formation law, demonstrating that feedback processes are more important in regulating the stellar mass than the precise star formation law itself.

*Key words:* Galaxy: formation – Galaxy: evolution – methods: numerical

## 1. Introduction

The study of galaxy structure, encompassing attributes such as galaxy radius, thickness, and morphology, is pivotal in astrophysics, offering profound insights into the processes of galaxy formation and evolution. Observational astronomy has made significant strides forward with modern galaxy surveys such as the Sloan Digital Sky Survey (SDSS), Dark Energy Survey and Large Synoptic Survey Telescope and advanced instrumentation such as the Hubble Space Telescope and James Webb Space Telescope (JWST), which have provided a wealth of data on the properties and distribution of galaxies across the universe (Shen et al. 2003). The observations are crucial for understanding the diverse forms that galaxies can take and how these forms change over cosmic time (Conselice 2014). Parallel to observational efforts, computational simulations have become an indispensable tool in astrophysics, providing a powerful way to study and predict the complex processes that influence galaxy formation. Projects like Illustris (Vogelsberger et al. 2014b) or EAGLE (Crain et al. 2015) have been at the forefront of these efforts and ushered in the possibility to study whole galaxy populations with hydrodynamical simulations. These calculations employ sophisticated but still approximate models to simulate the physical processes governing galaxy evolution within the cosmological context. They are designed to mirror the universe's evolution under the influence of both dark matter and baryonic matter, and by doing this they offer insights into phenomena that are challenging to observe directly.

Despite these advances, significant discrepancies remain between the results of simulations and observational data, particularly concerning the radius, thickness, and overall morphology of galaxies. For instance, simulations often struggle to accurately reproduce the scale lengths and disk thicknesses observed in spiral galaxies (Crain et al. 2015;

Pillepich et al. 2018b). Additionally, the morphological diversity of galaxies, particularly the detailed structure of spiral arms and the bulge-to-disk ratios in different galaxy types, frequently does not match observational results (Genel et al. 2014). Understanding and resolving these discrepancies are therefore important goals in the field. This is because the disparities between observed and simulated galaxies can indicate fundamental gaps in our understanding of physical processes such as star formation, its regulation by feedback mechanisms, and the role of dark matter in galaxy evolution (Hopkins et al. 2014; Naab & Ostriker 2017). Moreover, as theoretical models inform both observational strategies and interpretations, inaccuracies in simulations can lead to broader misconceptions about the structure and history of the universe. Therefore, bridging the gap between simulation and observation is not merely a technical challenge but a fundamental necessity to advance our understanding of the physics of galaxy formation and our ability to validate our overall cosmological model.

One of the most persistent issues in cosmological simulations is their struggle to accurately reproduce the observed radii and scale-heights of galaxies. Observational data, such as those from the SDSS, have provided detailed statistics on the distribution of galaxy sizes across different galaxy types and redshifts (Shen et al. 2003). However, simulations often predict galaxies that are either too compact or too extended compared to real galaxies. For instance, the Illustris project, despite its sophisticated treatment of galaxy physics, has shown difficulties in matching the size distribution of low-mass galaxies, often resulting in galaxies that are too dense (Genel et al. 2014). Similarly, the EAGLE simulation, while improving the match in galaxy size at higher masses, still shows discrepancies at lower galaxy masses (Furlong et al. 2017). These mismatches suggest that additional factors, such as feedback efficiency from star formation and supernovae, may not be accurately modeled in these simulations.

The thickness of galaxy disks presents another challenge. Observations indicate a variety of disk thicknesses across different galaxy types, influenced by factors like stellar age, gas content, and environmental interactions. Nevertheless, simulations have traditionally struggled to replicate these features accurately. For example, many simulated disk galaxies tend to be thicker and less differentiated in their vertical structure compared to observations (Grand et al. 2017). This issue points to potential shortcomings in how simulations handle processes such as the heating and cooling of the interstellar medium (ISM), the impact of dark matter, and the dynamics of stellar populations. In the same vein, the formation of realistic spiral structures and bars in simulated galaxies has been met with significant difficulty, often requiring higher resolution and better treatment of stellar feedback mechanisms to achieve more realistic results (Guedes et al. 2011). Additionally, the role of environment in shaping galaxy morphology, which is evident in observational surveys, is not always clearly replicated in simulations, suggesting a potential gap in our understanding of the processes that drive galaxy evolution (Moore et al. 1996).

These tensions between simulations and observations highlight some of the limitations of current theoretical models and call for work on refining the simulations. In particular, we note that one of the currently most successful cosmological simulation models, IllustrisTNG (Pillepich et al. 2018b), relies on a simple, heuristic equation of state model for the ISM that goes back to a coarse subgrid model of Springel & Hernquist (2003). Meanwhile, high-resolution simulation models of the ISM, such as SILCC (Kim & Ostriker 2017), which models the life cycle of molecular clouds, and TIGRESS (Walch et al. 2015; Girichidis et al. 2016), which simulates the three-phase ISM in galaxies with star formation and supernova feedback, have now achieved the capability to fully resolve how supernova-driven turbulence regulates star formation. Interestingly, these simulation projects can be used to measure average relations between the pressure and the gas surface density in the star-forming ISM. This thus yields effective equation of state models, essentially from first principles (Ostriker & Kim 2022), and which are thus physically better justified than the prescriptions in TNG. In this study, we aim for an initial investigation of the changes that can be expected when the ISM equation of state and star formation law in IllustrisTNG are replaced with expectations from these high resolution ISM simulations.

To this end we will first investigate idealized scenarios within a tall box to study the vertical structure of self-gravitating gaseous sheets, which is a model for a small patch in a disk galaxy. We then turn to applying the two models to fully cosmological simulations of disk galaxy formation. For definiteness, we adopt 12 models of Milky Way-sized galaxies taken from the Auriga project for this purpose. We are particularly interested in whether a change of ISM equation of state has an impact on the radial and vertical structure of the formed galaxies.

This paper is structured as follows. We first describe in Section 2 the details of the two ISM and star formation models we apply. In Section 3 we validate their implementations in a series of tall box simulations, allowing us, in particular, to investigate the expected vertical structure of star-forming gaseous layers in disk galaxies for different surface densities. We then turn in Section 4 to studying fully cosmological simulations of the formation of Milky Way-sized galaxies with initial conditions taken from the Auriga project. We compare results for 12 different galaxies models, each run with our two ISM treatments. Our analysis focuses on differences in the radial galaxy structure, in the star formation properties, and in the vertical structure of the simulated galaxies. Finally, we discuss our results and present a summary of our conclusions in Section 5.

## 2. Methodology

In this section, we first specify the ISM model applied in the IllustrisTNG simulation project and then contrast this with the results obtained in recent high-resolution simulations of the ISM in the TIGRESS project, as concisely summarized by Ostriker & Kim (2022) in terms of fitting functions. We shall use the latter as a basis to formulate a simple alternative model to TNG, which we then study in the rest of the paper.

The IllustrisTNG project consists of a suite of cosmological galaxy formation simulations that build upon the foundations laid by its predecessor, the original Illustris simulation (Vogelsberger et al. 2014a). IllustrisTNG, or simply TNG for brevity, has been launched to address and improve upon the limitations of the earlier Illustris model. TNG incorporates a comprehensive suite of physical processes and refines the treatment of phenomena such as star formation, magnetic fields, black hole growth, and feedback mechanisms (Nelson et al. 2018; Pillepich et al. 2018a). The model operates within the cosmological framework provided by the ΛCDM theory, and utilizes state-of-the-art numerical techniques, specifically the moving-mesh code AREPO (Springel 2010), to simulate large volumes of the universe across cosmic time. One of the key features of IllustrisTNG is its improved handling of galactic winds and stellar feedback, which are crucial for accurately modeling galaxy sizes and star formation rates. Additionally, the model integrates advanced algorithms for magnetohydrodynamics, which are essential for studying the influence of magnetic fields on galaxy formation and evolution (Weinberger et al. 2017). The success of IllustrisTNG in producing realistic, diverse galaxy populations has made it an extremely valuable tool for studying the physical processes that shape galaxies and their observable properties.

The treatment of the star-forming ISM in IllustrisTNG relies on a subgrid model originally proposed by Springel & Hernquist (2003). In this approach, the ISM is pictured as a two-phase medium composed of cold clouds at specific thermal energy per unit mass $u_c$, and a diffuse hot phase at thermal energy $u_h$, and with spatially averaged mass densities $\rho_c$ and $\rho_h$, respectively. The effective pressure of the medium is then given by

$$P_{\rm eff} = (\gamma - 1)(\rho_h u_h + \rho_c u_c), \tag{1}$$

where $\gamma = 5/3$ is the adiabatic index for the gas. Assuming that clouds are formed by radiative cooling, are partially consumed by star formation, and destroyed by supernova feedback, and by making some further simplifying assumptions, Springel & Hernquist (2003) derived how $P_{\rm eff}$ depends on the total mass density of the gas, provided the gas density is above a threshold density $\rho_{\rm th}$ for star formation. This effective equation of state, $P_{\rm eff} = P_{\rm eff}(\rho)$, can be described by a fitting formula (in cgs units) given by Robertson et al. (2004) as

$$\log P_{\rm eff} = 0.05(\log n_{\rm H})^3 - 0.246(\log n_{\rm H})^2 + 1.749 \log n_{\rm H} - 10.6, \tag{2}$$

where now $n_{\rm H}$ is expressing the density in terms of the number density of hydrogen atoms.

The equation of state described by the Springel & Hernquist (2003) model is comparatively stiff, yielding gas disks that are relatively thick and not particularly susceptible to producing spiral arms. As Springel et al. (2005, see their Figure 6) show, less strong effective pressure support can produce thinner disks that are more prone to develop perturbations such as spiral arms and bars. To allow for this possibility, the IllustrisTNG model adopted a heuristic model for a softer equation of state proposed by Springel et al. (2005) by interpolating between the model expressed in Equation (2), and an isothermal equation of state, $P_{\rm iso}$, with gas at temperature $10^4$ K (and a mean molecular weight corresponding to full ionization). A simple linear average

$$P_{\rm TNG} = q_{\rm EOS} P_{\rm eff} + (1 - q_{\rm EOS}) P_{\rm iso}, \tag{3}$$

with $q_{\rm EOS} = 0.3$ then defines the IllustrisTNG equation of state.

Besides the effective equation of state, the ISM model also describes the process of star formation, at a rate motivated by observations (Kennicutt 1989, 1998). This is taken to be

$$\frac{d\rho_*}{dt} = (1 - \beta)\frac{\rho_c}{t_*}, \tag{4}$$

where $\frac{d\rho_*}{dt}$ is the local star formation rate, $\beta$ is the mass fraction of stars that die immediately as supernovae, $\rho_c$ is the mean density of cold gas, and $t_*$ sets the characteristic timescale of star formation. Both in Springel & Hernquist (2003) and the TNG model, the density dependence of the characteristic timescale is parameterized as

$$t_*(\rho) = t_*^0 \left(\frac{\rho}{\rho_{\rm th}}\right)^{-1/2}, \tag{5}$$

where $t_*^0$ is a constant parameter, $\rho$ is the total gas density and $\rho_{\rm th}$ is the threshold density for star formation.

As mentioned earlier, modern high-resolution simulations of the ISM (e.g., Ostriker & Shetty 2011; Kim et al. 2013) have revealed that the star-forming medium is not a simple two-phase medium, but has a much more complicated structure in which supersonic turbulence driven by supernova explosions plays a crucial role. In particular, this feedback loop is important for understanding the efficiency and distribution of star formation across different galaxy environments. The theoretical analysis of Ostriker & Kim (2022) has shown that the pressure in the ISM regulates itself such that it balances the gravitational weight of the gas in a star-forming disk, with feedback effects modulating the star formation rate just to the right level to achieve an overall dynamical balance between

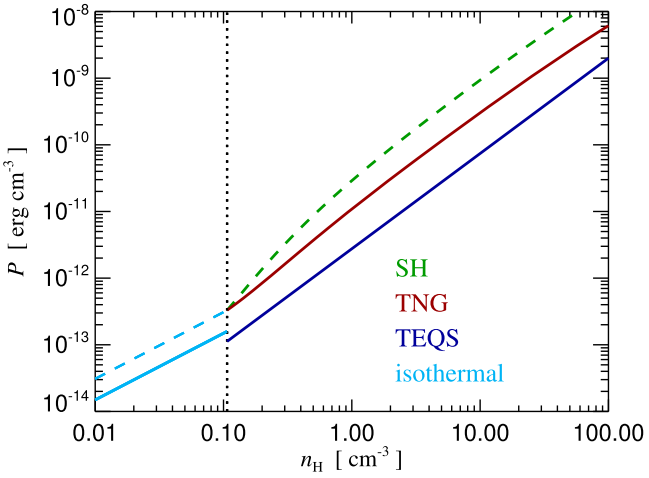


**Figure 1.** Effective equation of state for the two models we study here: The red line corresponds to the TNG model, while the dark blue line is our TEQS model, which is based on the average relation between pressure and gas density found in high-resolution ISM simulations that include resolved supernova feedback (Ostriker & Kim 2022). For comparison, we also include the equation of state of the original Springel & Hernquist (2003) model (green dashed). The TNG model is defined as a linear interpolation between this model and an isothermal equation of state (dashed blue line). These equations of state models are applied by the code above the star formation threshold of $n_{\rm H} \simeq 0.1$ cm$^{-3}$ (vertical dotted line). The light blue lines stand for isothermal equations of state at $10^4$ K, either assuming fully neutral (solid line), or fully ionized gas (dashed line). For densities just below the star formation threshold, most of the gas in cosmological simulations is at a temperature of $10^4$ K and is neutral, but some can also have a higher ionization state.

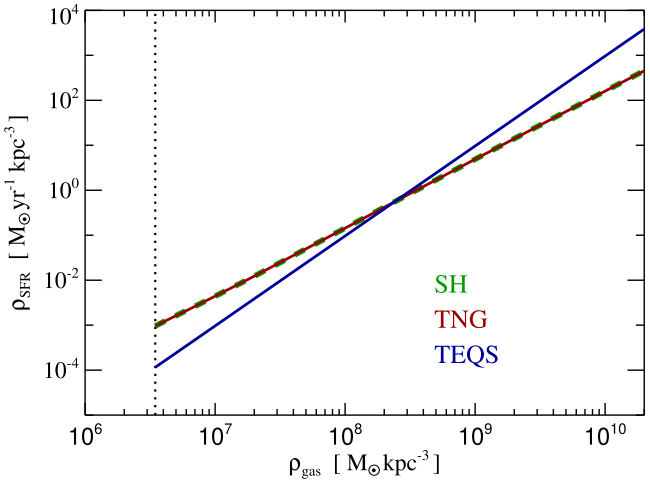


**Figure 2.** Our adopted relationships between the star formation rate per unit volume and the gas density in the TNG (red) and TEQS (blue) models, as labeled. The TNG model here coincides with the Springel & Hernquist (2003) model (green dashed), whereas the TEQS model adopts a +0.5 steeper power-law slope in order to reproduce the relation between $\Sigma_{\rm SFR}$ and $\Sigma_{\rm gas}$ seen in the small-scale ISM simulations (see Figure 3).

turbulent pressure and gravity. The corresponding theory of pressure-regulated, feedback-modulated star formation can describe the results of these full physics simulations well.

Furthermore, despite the complexity of the ISM structure in these models, there is still a fair amount of regularity in the mean properties of the ISM. In particular, the simulations show a relation between the mean pressure and mean gas density, which can be fit with (in cgs units)

$$\log(P_{\rm eff}) = 1.43\,\log(n_{\rm H}) + 4.30. \quad (6)$$

In addition, if the vertical gravity is dominated by the gas, there is also a power-law relation between the gas surface density and the surface density of star formation (Ostriker & Kim 2022), which is given by

$$\Sigma_{\rm SFR} \propto \Sigma_{\rm gas}^2. \quad (7)$$

We make these two relations the basis of an alternative parameterization of the ISM subgrid model in our simulations, which we here call "TEQS," for TIGRESS-inspired equation of state.

The study by Ostriker & Kim (2022) does not explicitly specify a three-dimensional star formation law that we however need in our sub-grid treatment. However, we find that slightly steepening the star formation timescale dependence, to

$$t_*(\rho) = t_*^0 \left(\frac{\rho}{\rho_{\rm th}}\right)^{-1}, \quad (8)$$

is required and sufficient to reproduce the surface density relation of Equation (7). This is the second component in our TEQS model, and Equations (6) and (8) replace the corresponding versions (5) and (3) of the TNG model, together with a small adjustment of $t_*^0$ to match the TIGRESS results. Other than that, there are no changes to the radiative cooling and stellar/AGN feedback models compared to IllustrisTNG.

In Figure 1 we illustrate the different effective equations of state of these models. The red line is for the TNG model while the blue line is for the TEQS model, and we also include the original Springel & Hernquist (2003, hereafter SH) model, for comparison. We clearly see that the IllustrisTNG prescription is already substantially "softer" than the SH model, i.e., its pressure is lower at any given density, and also the slope of the pressure–density relation is shallower. The TEQS model is however providing even lower pressure at the same density, and is slightly shallower still. This means that there is less resistance to gravity, and we expect that a given amount of gas under self-gravity is compressed to higher densities by this model.

In addition, we have adopted a different dependence of the star formation rate on gas density, as displayed in Figure 2. The steeper relation we have adopted for TEQS favors star formation in denser gas but reduces star formation in less dense gas. We have adopted this change in order to obtain a steeper relation between the star formation surface density and

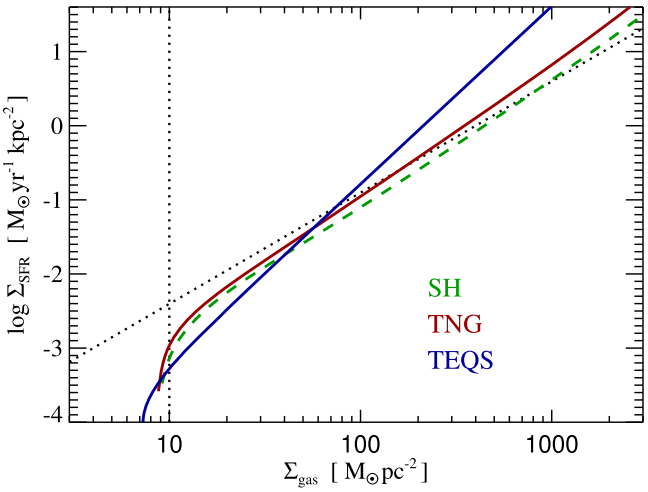


**Figure 3.** Expected relationship between the surface density of star formation and the total gas surface density for the equation of state and star formation models considered here (red for TNG, and blue for TEQS). For comparison, the dotted inclined line marks the star formation law inferred observationally from Kennicutt (1998), as well as the observationally inferred cut-off density (vertical dotted line), to which the original Springel & Hernquist (2003) model (dashed green) was calibrated. The TNG model has slightly higher star formation than SH at the same surface density because its softer equation of state allows higher gas densities at the same surface density.

gas surface density in self-gravitating sheets of star-forming gas, which can serve as a simple model for a small patch of a star-forming disk, ignoring for the moment the possible presence of an additional stellar disk component. In this case, one can solve for the hydrostatic equilibrium of the gas layer under the pressure law given by the effective equation of state, and then integrate the implied star formation rate in the sheet.

The result of this calculation is shown in Figure 3, both for the TNG and the TEQS models. The TEQS parameterization produces something that quite closely matches the behavior seen in Ostriker & Kim (2022) for their high-resolution ISM simulations of gaseous layers without stars, as desired. Utilizing these two models, it will therefore be interesting to see whether there are any important consequences for simulations of galaxy formation. After all, the TEQS model is in principle better justified on physical grounds as it is directly calibrated on small-scale full-physics calculations, whereas TNG is based on a heuristic modification of a much coarser model. To investigate this question, we will in the following first examine simulations of gaseous sheets within a tall box under idealized conditions, and then apply the models to full cosmological simulation of the formation of Milky Way-sized galaxies.

## 3. Tall Box Simulations

To validate the implementation of our new equation of state and star formation subgrid model in the moving mesh-code AREPO (Springel 2010; Weinberger et al. 2020), and to elucidate its impacts on the vertical structure of star-forming layers of gas, we here first construct several tall box simulations that can be used to mimic infinitely extended sheets of material.

### 3.1. Simulation Setup

We consider a tall box with dimensions of 1 kpc in both $x$- and $y$-directions, and 32 kpc along the $z$-axis. The simulation volume has periodic boundary conditions in the $x$- and $y$-directions, and open boundary conditions in the $z$-direction, which apply both to hydrodynamics and self-gravity of the gas in the box. Besides this, radiative cooling, star formation and feedback are enabled, but we prevent the simulation code from actually spawning new star particles so that we can study the equilibrium of the setup over a longer timescale without actual consumption of the gas.

We fill in gas at the mid-plane of the $z$-axis, with a prescribed surface density and a profile that is expected to be in equilibrium for the chosen equation of state model. We utilize three sets of gas surface densities, with values of $\Sigma_{\rm gas} = 20$, 100, and $500\,M_\odot$ pc$^{-2}$. These gas sheets are realized with mesh-generating points that sample the profile, giving constant mass resolution within the sheet. The rest of the volume of the tall box is filled with a very low background density component, a step that is necessary for the moving-mesh code AREPO because space cannot be simply empty but must always be tessellated by some kind of mesh.

We then evolve the simulations both with the TNG and the TEQS models, for a timespan long enough that ensures that any residual initial perturbations (which turn out to be extremely small for our initial conditions) have damped out. The gaseous sheets are then in a quasi-stationary state that we illustrate in Figure 4 by displaying the mesh-generating points for a thin slice through the tall box of depth 1/10th of the total thickness of the box. We can readily see that the TEQS model produces substantially thinner gaseous layers at a given surface density compared with TNG. This is because the softer equation of state requires the gas to be compressed to higher density before its ISM pressure can match the self-gravity of the gas. Similarly, for higher gas surface densities, the thickness of the star-forming gaseous sheet becomes progressively thinner.

### 3.2. Gas and Star Formation Profiles

We now examine the resulting equilibrium profiles in more detail. In Figure 5 we compare the structure of the gas profiles for the three surface densities we examined, each displayed in a separate panel. The direct comparison of TNG and TEQS quantitatively confirms the visual impression we obtained earlier. For the same surface density (implying equal areas underneath the curves in these plots), the TEQS always produces thinner gaseous layers. Note that this can have important consequences for the dynamical stability of

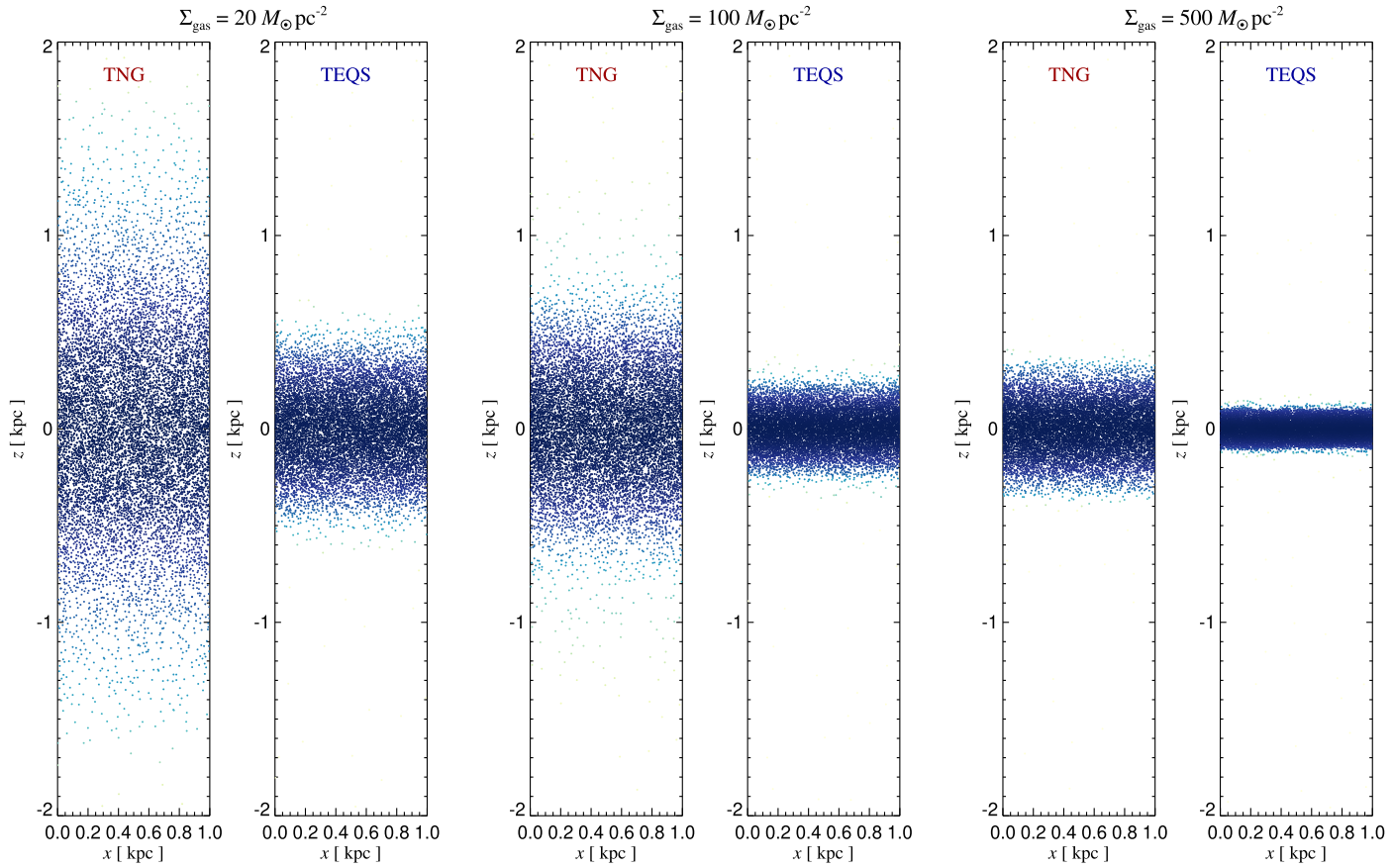


**Figure 4.** Gas stratification in tall box simulations for three different gas surface densities, as labeled, comparing our two different equation of state models, TNG (left) and TEQS (right). We show the mesh-generating points in a side-view of a thin slice through the box, focusing on the central region (the total height of the box is 32 kpc).

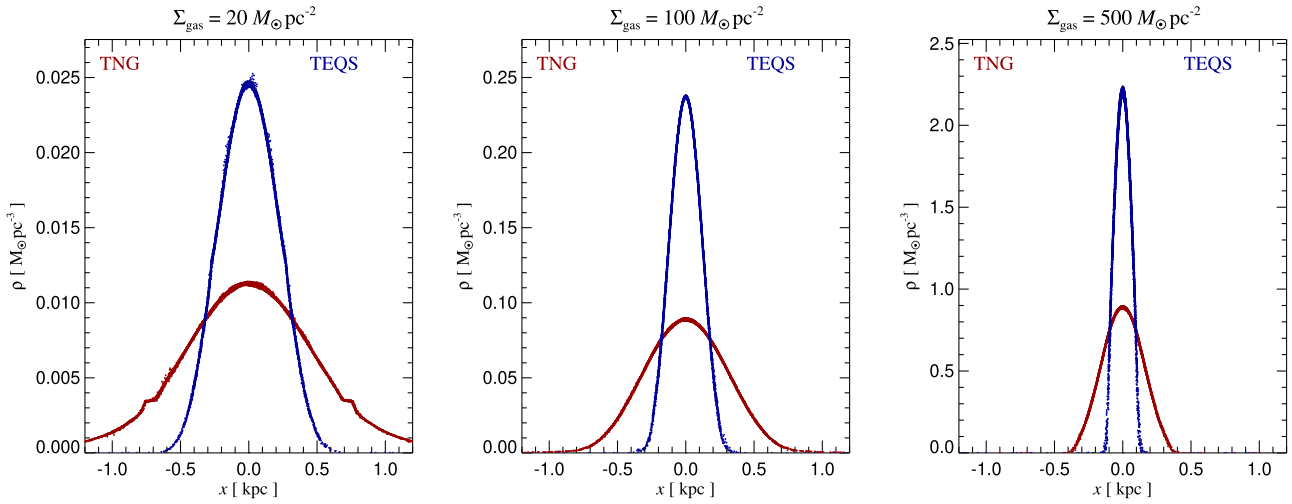


**Figure 5.** Gas density profiles of our tall box simulations for different gas surface densities (as labeled), comparing our two different equation of state models, TNG (in red) and TEQS (in blue).

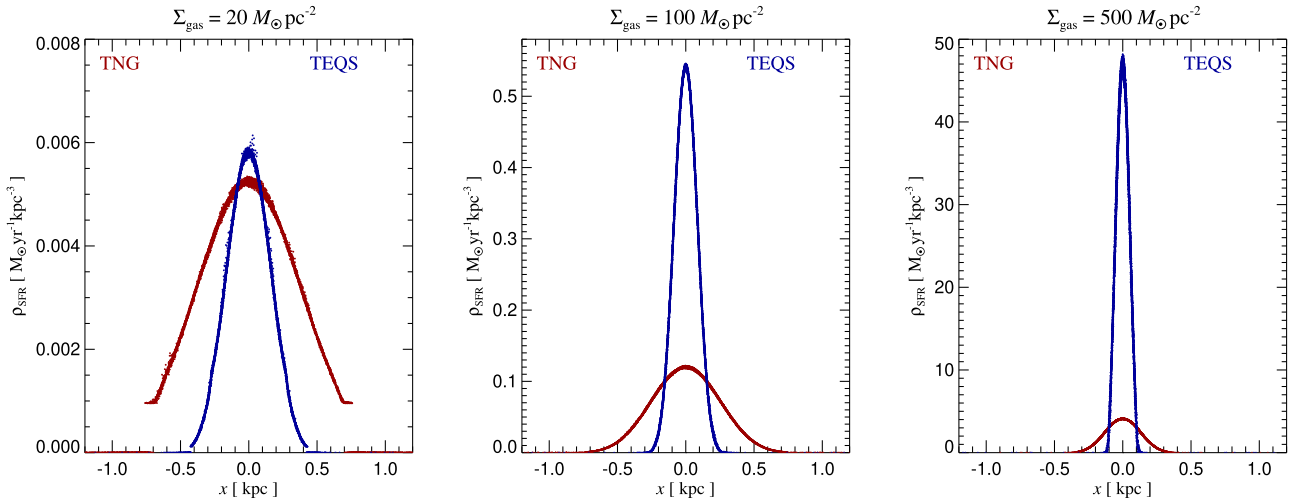


**Figure 6.** Vertical profile of the star formation rate density in our tall box simulations, for three different gas surface densities, as labeled. We show results for the TNG (red) and TEQS (blue) models. Note that the measurements for TNG at the lowest surface density start at finite star formation density because here the gas density drops below the density threshold for star formation.

differentially rotating disks, where we expect the thinner layers to be more susceptible to various types of perturbations.

Since these gaseous layers are star-forming, we consequently also expect that the produced stellar distributions will have different thicknesses for the two equation of state models. We can get a sense for this by considering the instantaneous star formation profile, which is directly proportional to the stellar mass density produced during some short time interval. These profiles are shown in Figure 6, again comparing TNG and TEQS for the three gaseous surface densities in different panels. Here the area underneath the curves is proportional to the total star formation rate surface density. Interestingly, this is lower in the TEQS model than in TNG for the low surface density of $\Sigma_{\rm gas} = 20\,M_\odot$ pc$^{-2}$, whereas for the higher surface densities the TEQS model has higher star formation overall than TNG. This is a result of the steeper star formation law of TEQS compared with TNG, which favors higher densities. The shapes of the star formation rate profiles in TEQS are therefore even narrower than those in TNG, but both are already narrower than the gas density profiles themselves. In principle, we would therefore expect the TEQS model to produce thinner stellar disks than TNG if all other things are equal, and provided vertical heating processes for the stellar disk are sufficiently subdominant so that the intrinsic initial thickness can be preserved. Whether this applies in cosmological simulations is unclear, but we will take a look at this in the next section.

## 4. Milky Way-sized Simulations

### *4.1. Auriga Initial Conditions*

To test the impact of the new equation of state model in cosmological simulations we focus on the mass scale of Milky Way-sized galaxies, i.e., we consider zoom-in simulations of halos of mass $\sim 10^{12}\,M_\odot$. For convenience, we utilize initial conditions of the Auriga project (Grand et al. 2017), which is a comprehensive and successful series of studies that primarily focuses on the formation and evolution of Milky Way-like galaxies within a cosmological context. The project carried out high-resolution magnetohydrodynamical simulations with the AREPO code, using a predecessor to the physics model employed in IllustrisTNG. The Auriga physics model is however very similar to TNG in practice, only the treatment of black hole radio-mode feedback varies significantly, but this difference only becomes important for more massive halos. Here we in any case re-run the initial conditions with the TNG physics model, and compare the results to a second set of simulations which employ the TEQS model. We can then compare the resulting galaxies in a pair-wise fashion.

In our study, we adopt a subset of galaxies from the Auriga project, more specifically we have picked 12 simulations designated Au2, Au3, Au6, Au9, Au12, Au14, Au17, Au18, Au24, Au26, Au27, and Au28 in the original Auriga project. We focus on the default resolution level-5, which corresponds to a baryonic mass resolution of approximately $5 \times 10^4\,M_\odot$, and a dark matter mass resolution of $3 \times 10^5\,M_\odot$. All simulations were carried out with the current version of the AREPO code, using standard integration settings and the physics model parameter settings corresponding to IllustrisTNG. The cosmological parameters for the simulations match those of the parent simulation for which the zoom-in initial conditions were constructed, which is actually the EAGLE simulation box. They are $\Omega_m = 0.307$, $\Omega_b = 0.048$, $\Omega_\Lambda = 0.693$, and a Hubble constant value of $H_0 = 100\,h$ km s$^{-1}$ with $h = 0.6777$.

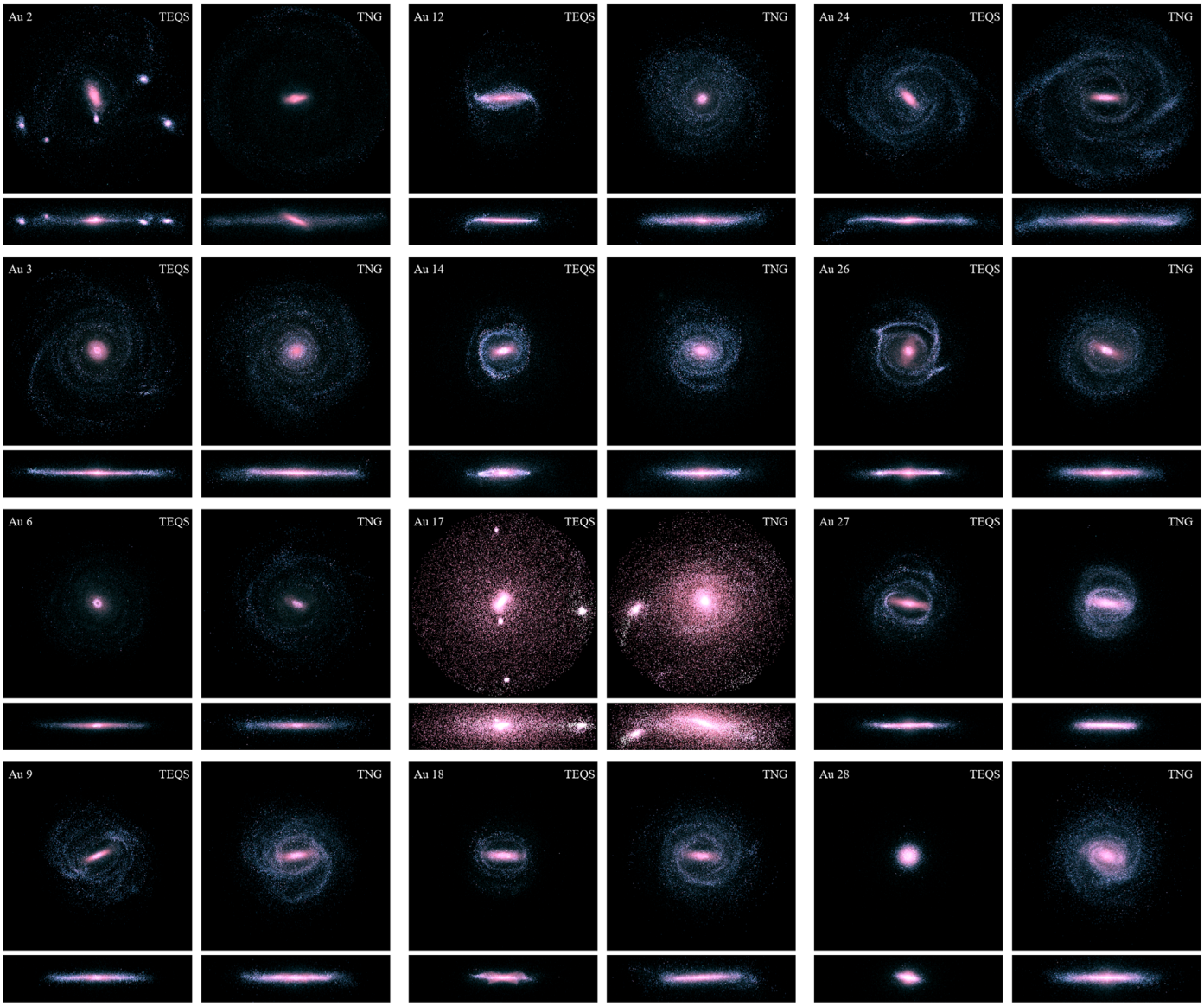


**Figure 7.** Galaxy images of the stellar distributions in our re-simulations of 12 models taken from the Auriga set of initial conditions. Each pair of images shows the same galaxy, but simulated on the left with the TEQS model, and on the right with the TNG model. In each case, face-on views are given in the panel on top, and an edge-on view is shown in the panel on the bottom.

### *4.2. Morphology and Total Stellar Mass*

In Figure 7, we provide a visual comparison of our simulation pairs, in the form of face-on and edge-on views of the stellar distributions of the disk galaxies at $z = 0$. The left half of each pair gives the results for the new TEQS model whereas the right half displays the corresponding TNG simulation. From the images, it can be observed that the two groups of simulations exhibit a certain degree of pair-wise similarity, yet the differences between each pair within the sample are still significant. Sometimes the disks appear larger in TEQS and bars are more prominent, sometimes the opposite can be observed. Clearly, there is large system to system variation between the response of the galaxies to the modification of the equation of state model, without a clearly discernible universal trend. We will thus need to consider the average impact on the structural properties averaged over the sample of galaxies, something that we will pursue below.

Before getting to this, it is however also interesting to consider global integral properties of galaxies, with the most important being their total stellar mass. We look at this in Figure 8, where we show the stellar mass of each TNG galaxy (sold circles) and contrast this with the stellar mass found for

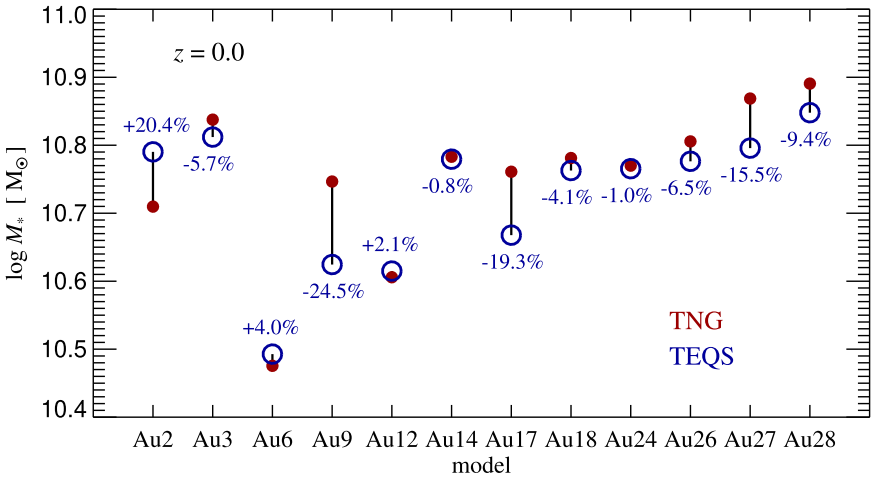


**Figure 8.** Stellar masses of the 12 galaxy initial conditions simulated with the TNG and TEQS models for the ISM equation of state and the star formation law. The stellar masses are surprisingly insensitive to this modeling choice, considering also that some stochastic variations are expected even if the same simulation was repeated multiple times. There is a hint that the TEQS stellar masses may be slightly smaller on average; for our sample, the average difference corresponds to a reduction of ≃6%.

the corresponding galaxy simulated with TEQS (hollow circles). We also include numerical values for the relative difference between the stellar masses directly in the figure. In general, the stellar masses are quite robust between the two models, especially given that it is known that even an identical model is subject to scatter when it is rerun, for example, with a changed random number seed (the spawning of new start particles is modeled as a stochastic process), simply due to the highly nonlinear nature of the evolution. The averaged change we find is a reduction of about 6% of the stellar mass when going from TNG to TEQS. This is small enough that we consider it to be within the noise. So to first order, there is no significant change in the stellar mass due to the use of the different equation of state and star formation law model.

### *4.3. Radial Galaxy Structure*

We now consider the stellar density distribution of our simulated galaxies in more detail. In the left panel of Figure 9, we illustrate the stellar surface mass density variations with radius, where the solid lines represent simulations from the TEQS model, while the dashed lines give those from the TNG model. Matching pairs of simulations are drawn with different colors, and in each case, the galaxies are analyzed in a polar coordinate system that is aligned with the plane of their disks. For visual clarity, we use Au2 as a reference simulation and vertically offset each pair by factors of 10, 100, 1000, etc., to differentiate them more easily. It can be observed that, for the 12 simulation pairs shown in the figure, the central region's stellar surface mass density is generally much higher for the TEQS model than for the TNG model. However, as the radius increases, the surface stellar mass density in the TEQS model gradually levels off to match TNG at radii of several kpc, and then drops below that of the TNG model.

Next we consider the vertical structure of the stellar density distribution in the core region of the galaxies, i.e., along the symmetry axis of the galaxies, which is shown in the middle column of Figure 9. For these measurements we select a cylindrical region with a radius of 1 kpc centered on the galaxy's rotation axis. The results show that the TEQS model predicts for these central regions slightly higher density than TNG, which is generally consistent with our finding for the radial distribution. At the same time, with increasing distance from the center, the TNG model's surface stellar mass density gradually catches up to that found for the TEQS model so that for regions reasonably far from the galaxy's mid-plane, the differences in stellar surface density between the two models are not significant any more. Finally, in the right column of Figure 9, we examine the surface stellar mass density of the galaxy disk as a function of height above the disk. Specifically, we select an annular region between radii of 2 and 5 kpc to avoid the galactic core. We observe that, from the base up to 10 kpc above the disk plane, the stellar density in the TEQS model is almost always lower for each galaxy pair than that in the TNG model.

Hence, these results allow us to make a preliminary qualitative assessment: compared to the TNG model, stars in the TEQS model are more centrally concentrated toward the core region of the galaxy, yielding higher stellar density there, but without inducing significant differences in the thickness of the galaxy central region. At the same time, the stellar density in the outer disk region of TEQS models is lower than in TNG models, suggesting that both the radius and thickness of the galactic disk are smaller in TEQS than in TNG.

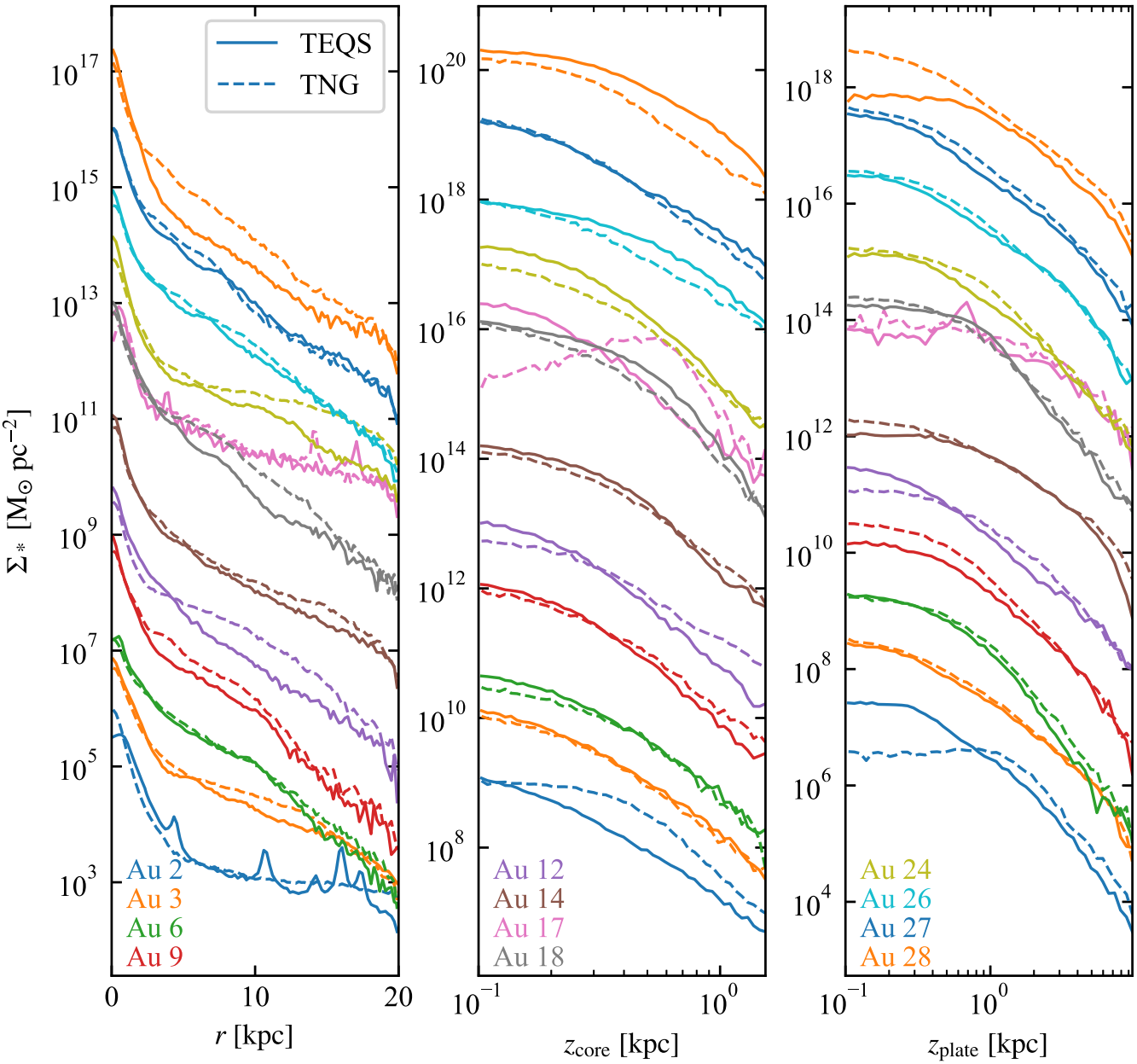


**Figure 9.** Stellar distributions of the full set of our galaxies, with Au2, Au3, Au6, Au9, Au12, Au14, Au17, Au18, Au24, Au26, Au27, and Au28 from bottom to the top respectively. The solid lines are for the TEQS model and the dashed lines are for the TNG model. Different colors signify different simulations, and we vertically offset each simulation by factors of 10, 100, 1000 etc. in the $y$-direction for visual clarity. Left panel: The radial stellar density distribution of all the galaxy simulations. The central region's surface stellar mass density in the TEQS model is generally much higher than that in the TNG model. However, as the radius increases, the surface stellar mass density in TEQS gradually levels off to match TNG at several kpc, and then falls below it. Middle panel: The axial density distribution in the core area. Here, we select a cylindrical region of radius of 1 kpc, centered on the galaxy's core, to compare the surface stellar mass density distribution along the symmetry axis. The results are generally consistent with the radial distribution. Right panel: The radial surface stellar mass density of the galaxy disk, specifically selecting an annular region between radii of 2 and 5 kpc. Within the range from the mid-plane up to 10 kpc above the disk, the stellar density in the TEQS model is typically consistently lower than that in the TNG model for each galaxy.

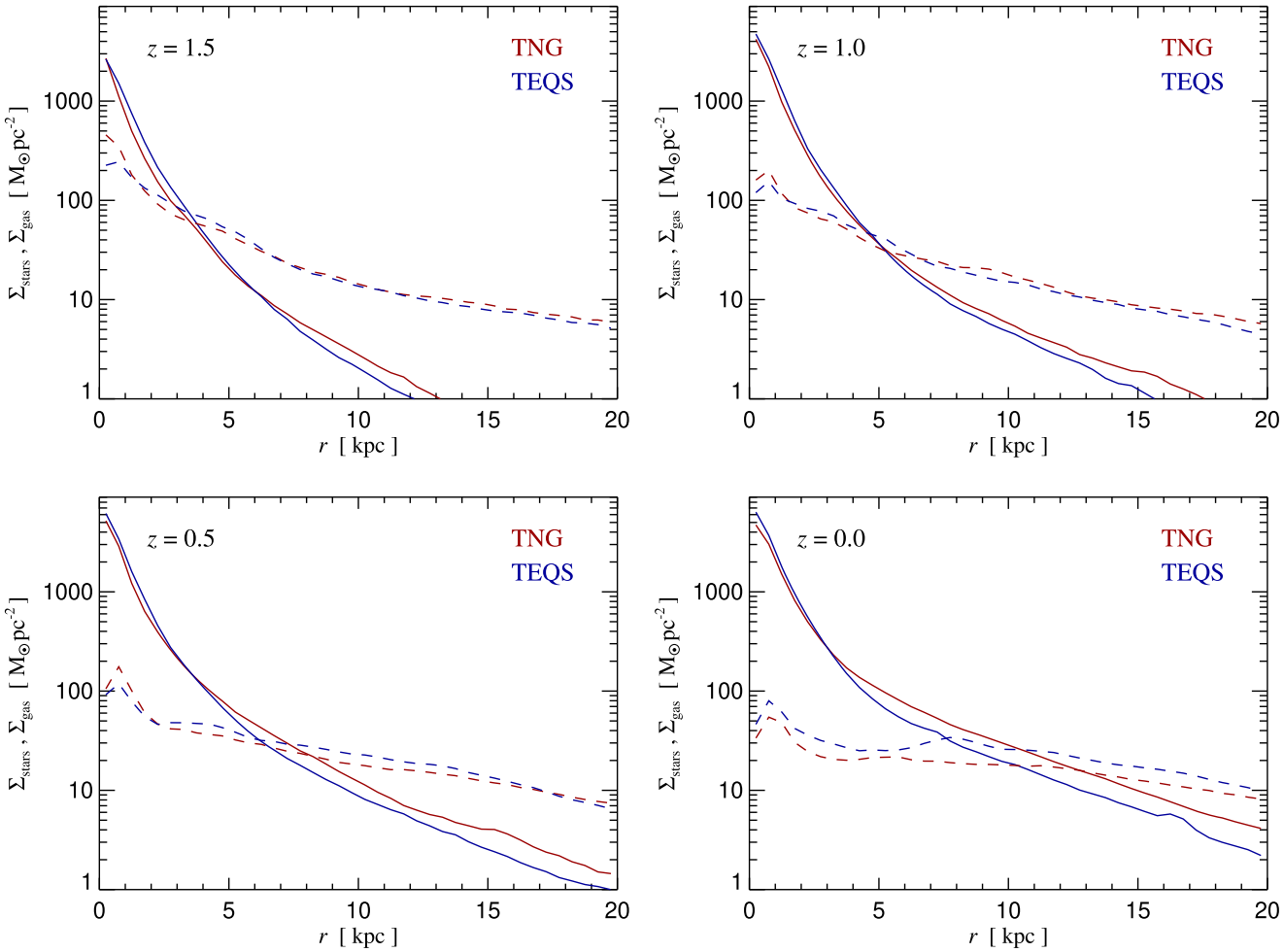


**Figure 10.** Averaged radial profiles of the stellar (solid) and gaseous (dashed) surface mass densities at different redshifts, as labeled, for our two equation of state and star formation models, TEQS (blue) and TNG (red).

To quantitatively back up this finding, we have calculated the radius and thickness of each simulation at different times. This involves measuring key parameters of the galaxies, namely the half-light radius, the effective radius, the effective thickness defined similarly to the effective radius, and the scale-height. The half-light radius $R_e$ is defined here as the radius within which half of the galaxy's total luminosity is emitted. It provides insight into the distribution of the light-emitting stars within a galaxy. The effective radius $R'_e$ is another measure of the size of a galaxy, indicating the radial extent within which 90% of the galaxy's total stellar mass is contained. This parameter is also useful for understanding the mass distribution and the extent of a galaxy.

The effective thickness $h'_e$ is defined similarly to the effective radius for better comparison. We again select a cylindrical region with a radius of 1 kpc centered on the galaxy's core to study the thickness. The scale thickness $h_z$ refers to the characteristic height of a galaxy, and is especially relevant for disk galaxies. We measure it perpendicularly to the plane of the galaxy so that it gives an idea of how "thick" or "thin" the galaxy appears. We define the scale-height by fitting the stellar profile with the formula

$$\rho(z) = \rho_0 \,\mathrm{sech}^2\left(\frac{z}{h_z}\right), \tag{9}$$

where $z$ is the vertical distance measured from the mid-plane of a galaxy's disk, $\rho(z)$ represents the density at height $z$, $\rho_0$ is the density at height $z = 0$, and $h_z$ denotes the scale-height of the disk. We again use a 1 kpc cylinder or ring for doing the relevant computation.

In Figure 10 we extend our analysis of radial surface density profiles by now showing stacked profiles of the 12 galaxies we simulated, both for the stellar mass and the gas mass, at redshifts $z = 1.5$, 1.0, 0.5, and 0. We have here computed simple unweighted averages of the measurements for the 12 systems, in order to highlight the mean behavior more clearly. The stellar profiles in the figure demonstrate the systematic

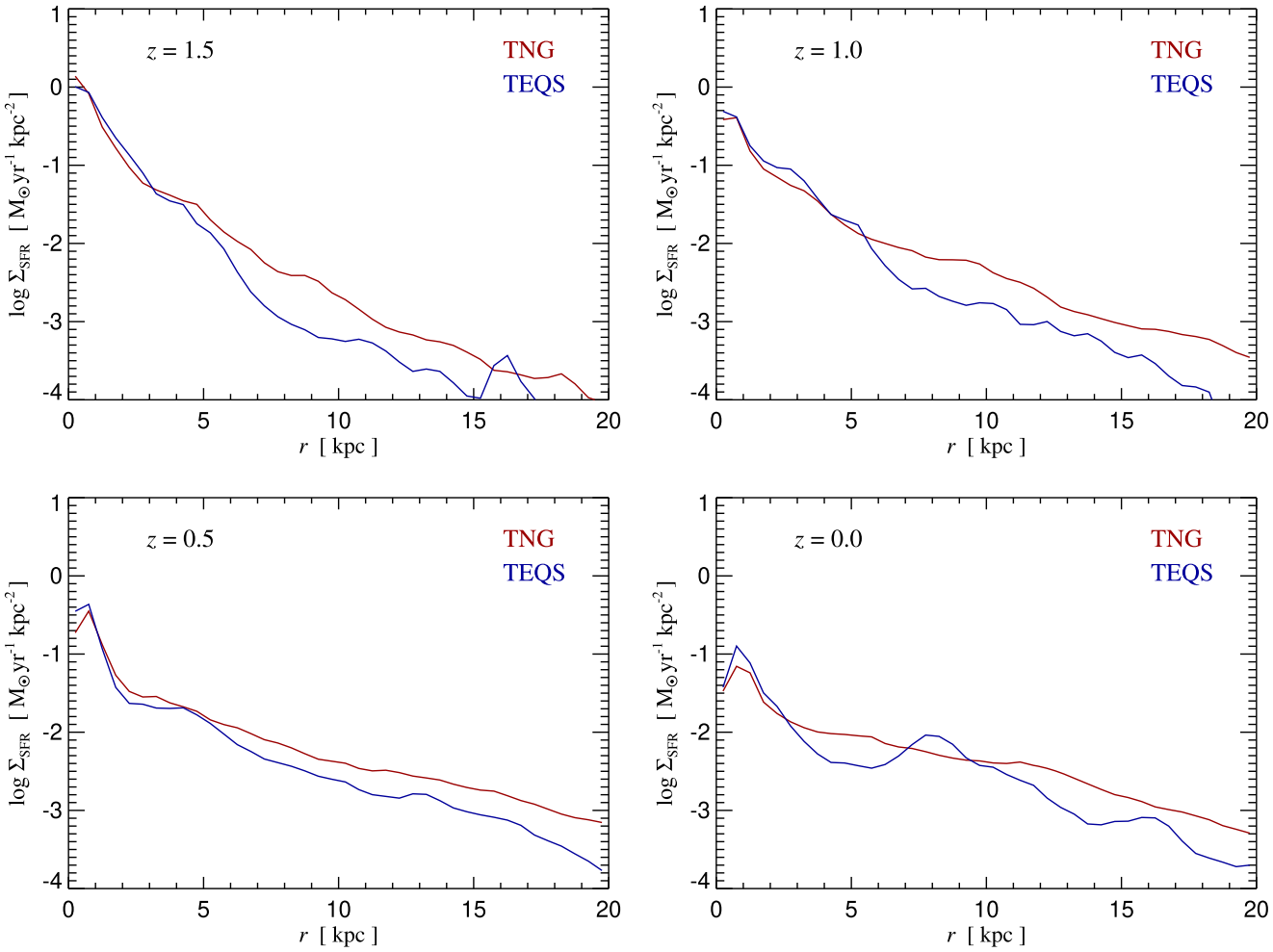


**Figure 11.** Stacked radial profiles of the star formation rate surface density, at different redshifts, for our two equation of state and star formation models, TEQS (blue) and TNG (red).

differences very clearly. The stellar density of the TEQS models tends to be higher in the inner parts, whereas in the outer parts the TNG model takes the lead. At intermediate radii, there is a crossing point, which approximately coincides with the place where the exponential outer profiles transition into a steeper "bulge" region. This behavior is found at all four examined redshifts, but the stellar profile grows with time, especially in the outer disk part, but less so in the inner regions.

Interestingly, the average gas surface density profile is much flatter, at $z = 0$ it is almost constant with radius. Here also the differences between TEQS and TNG are very small, and if anything, the gas density in the TEQS model tends to be slightly higher. Note also the opposite evolutionary trend of the gas density compared with the stellar distribution. The gas density, especially in the inner regions, declines with time, presumably reflecting the progressive gas consumption by star formation and the declining rate of gas accretion at late times.

### *4.4. Star Formation Properties*

In Figure 11, we now look at the radial profiles of the star formation rate densities, again stacking the 12 galaxy models we have simulated, separately for the TEQS and the TNG models. This allows us to get further insights into the origin of the radial structural differences, and whether this agrees with our expectations based on the properties of the two equation of state models. Again, we consider the four redshifts $z = 1.5$, 1.0, 0.5 and 0. We find a clear signature that the star formation rate density in the outer parts of the disks is on average lower for TEQS than for TNG. In the innermost regions, the trend reverses, also here the difference between TEQS and TNG is smaller. These findings are consistent with the stellar mass profiles we measured, i.e., the differences of the latter can be interpreted as naturally arising from variations in the star formation rate densities, and other possible explanations, for example a radial redistribution of stellar material, as a result of

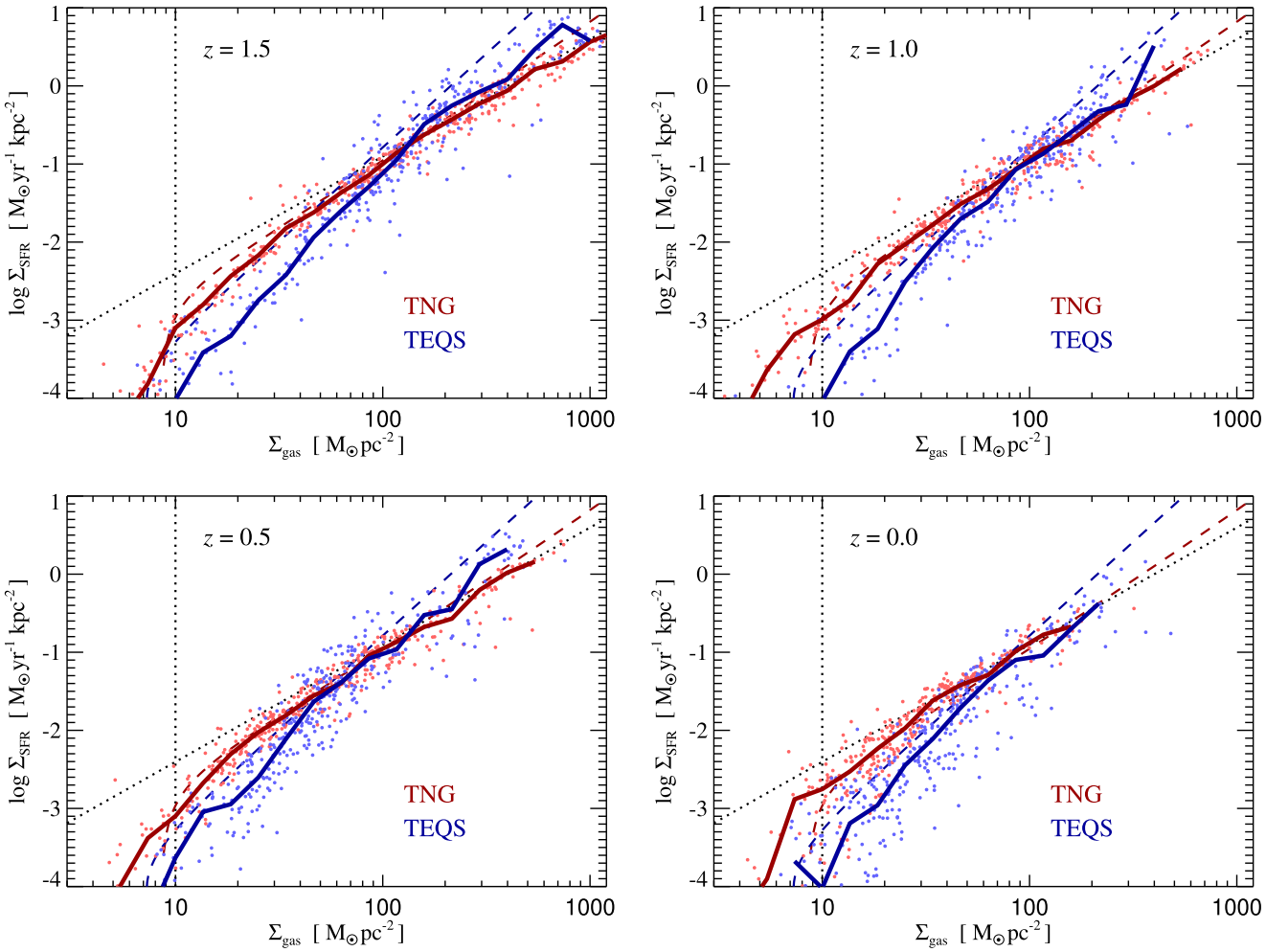


**Figure 12.** Relation between gas mass surface density and surface density of the star formation rate measured in our sample of Auriga simulations, at different redshifts, as labeled. For each panel we have determined the average gas density in logarithmically spaced azimuthal rings placed onto the plane of the disk. The thick lines (red for TNG and blue for TEQS) are running medians of the measurements for individual galaxies (points).

morphological differences, likely plays a subdominant or negligible role.

It is interesting to ask whether there is also a relation between the local gas surface density and local surface density of star formation, similar to the one we have drawn in Figure 3 for vertically stratified, self-gravitating gaseous sheets. To investigate this question we have placed concentric, logarithmically spaced cylindrical rings onto our 12 disk galaxies, and measured the gas surface density and the surface density of the star formation rate for each of them. The corresponding measurements are shown as dots in Figure 12, separately for the TEQS and TNG models, and for four different redshifts shown in different panels, as labeled. Thick lines are running medians for the data points. We also include the theoretically expected relations from Figure 3 for infinitely extended sheets, which are shown as dashed lines. Overall, the theoretically expected differences between TEQS and TNG are well reproduced—TEQS lies lower at lower gas surface densities, but then crosses over and is higher than TNG for the highest gas surface densities, or in other words, the TEQS relation is steeper than TNG. Both models are reasonably close to the theoretical expectation, even though this is not necessarily to be expected because actual disk galaxies are not really infinitely extended sheets, and so their structure is expected to be a bit different. Note however that the TEQS model shows somewhat larger differences than TNG relative to the expectation from an infinite sheet. This might indicate effects of resolution, as resolving the thinner disk structure of the TEQS model is harder than in TNG, and if resolution limitations broaden the vertical thickness of the gaseous layer the computed star formation rate would be biased low.

### *4.5. Vertical Galaxy Structure*

Using our measurements for the half-light radius, effective radius, effective thickness, and scale-height for each

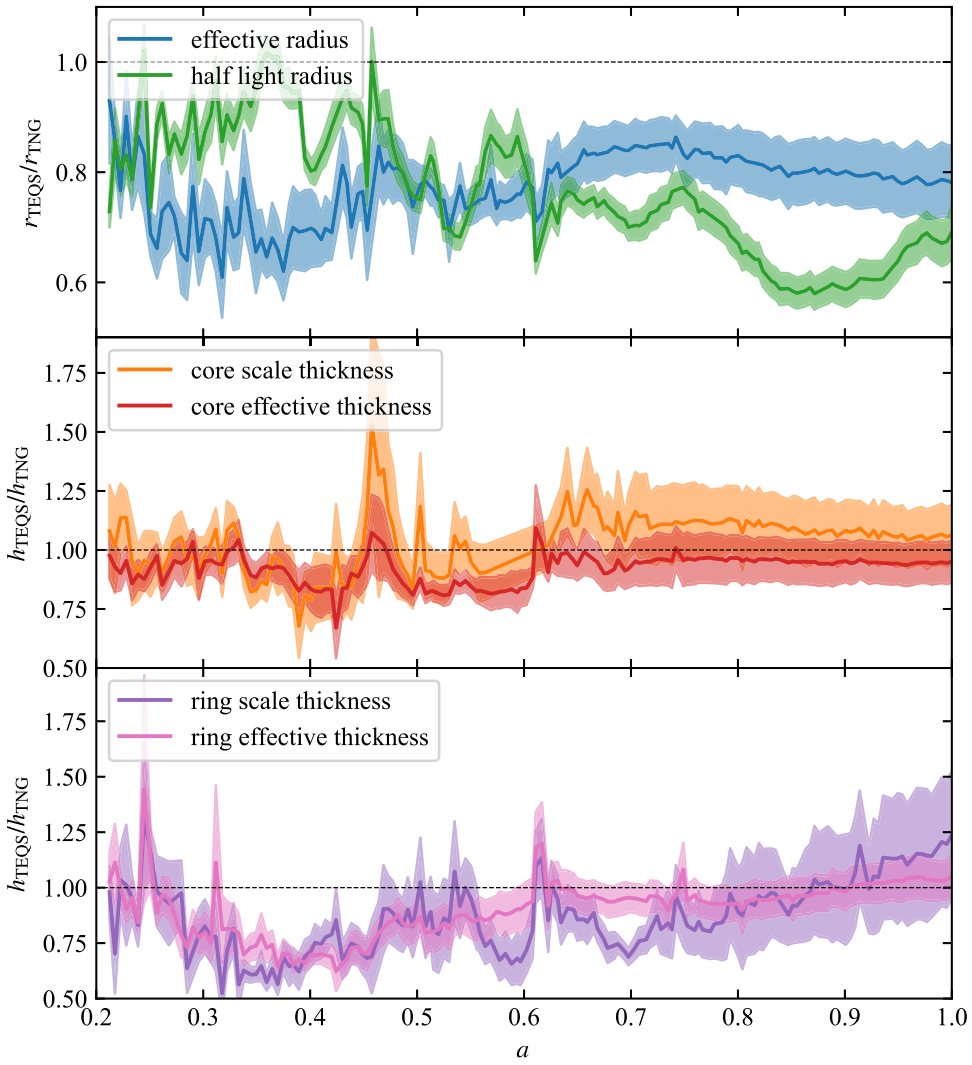


**Figure 13.** Comparison of the time evolution of different result between the TEQS and TNG models. In the top panel are the results for the effective radius and half light radius with standard error while the horizontal black line marks the equivalence of two models. For the galaxy radii—both for half-light radius and effective radius—the TEQS model consistently yields significantly smaller values compared to the TNG model, with the TEQS model's galaxy radii being about 20% smaller than those of the TNG model. The half-light radii show an even greater reduction, ranging from 30% to 40%. The middle panel gives the corresponding results for the thickness in the core region. The mean scale-height of galaxies in the TEQS model is slightly larger than in the TNG model, while the effective thickness is marginally smaller, but these differences are small compared with the uncertainties. The bottom panel also shows the disk thickness but this time in a ring region further out in the disks. No clear difference between the two models is found at early times, but at late times the TEQS model has a tendency to become slightly thicker than the TNG model, although this systematic difference is also within the errors.

simulation, we show in Figure 13 the temporal evolution of these quantities as a function of scale factor, from quite high redshift to the present time. We consider the ratio of these quantities between corresponding TEQS and TNG models, and show the averages for our sample of galaxies (solid lines), and also display the uncertainty of these means (shaded). The green line in the top panel of Figure 13 represents the half-light radius, while the blue line gives the effective radius. As anticipated from our earlier results, the TEQS model consistently yields significantly smaller values for half-light and effective radii compared to the TNG model, with TEQS galaxy radii being about 20% smaller than those of the TNG model. The half-light radii show an even greater reduction between 30% and 40%.

The red line in the middle panel of Figure 13 represents the effective thickness, and the yellow line gives the scale-height, with the shaded areas of the same colors indicating the standard error for each measurement. Here the measurements are done for the central regions of the galaxies. The differences in galaxy thickness are not nearly as pronounced as for the radii. In fact,

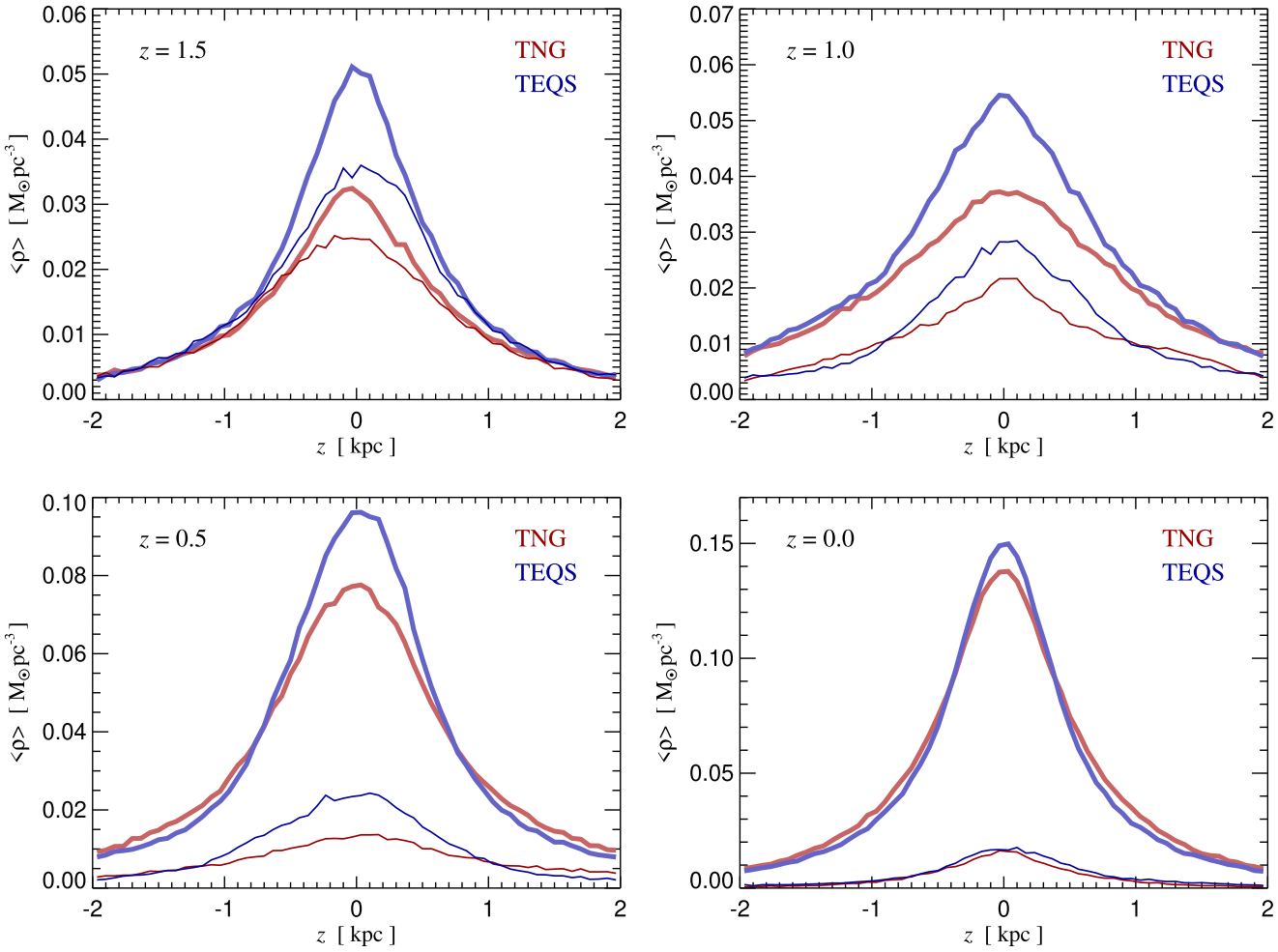


**Figure 14.** Vertical distribution of stars (thick lines), and gas (thin lines) at different redshifts for the TNG (red) and TEQS (blue) models. In this figure, we have carried out measurements in the radial range 2 to 5 kpc, and we stacked the results of all 12 simulated galaxies. Note that the vertical scale changes between the panels for the different redshifts; the stellar mass increases with time, whereas the gas mass declines. The TEQS model produces stellar distributions that are slightly more concentrated toward the mid-plane of the galaxies, but the effect is quite small.

the mean thickness of galaxies in their inner parts comes out slightly larger in the TEQS model than in the TNG model, while the effective thickness is marginally smaller, but these variations are within the measurement uncertainties. The slight variations related to the different definitions of galaxy thickness do not significantly impact the overall comparison, indicating that there is no substantial difference in the thickness at the cores of galaxies formed by the two models.

Finally, the bottom panel of Figure 13 repeats this comparison for a ring region in the exponential disk part of the galaxies. Similarly as for the central region, there is no clear difference between the two models at early times, but at late times the TEQS model appears to be slightly thicker than the TNG model. This is somewhat unexpected given our earlier findings for the tall box simulations, but again, these differences are small and lie within the measurement uncertainties, so they could be spurious. What is clear, however, is that the vertical distribution of stars does not appear to show substantial differences between the two models, unlike the radial distribution.

Figure 14 extends the analysis of the vertical structure of the galaxies by considering stacked profiles of the average gas density and average stellar density as a function of height $z$ above and below the mid-plane of the disk galaxies. We measure this in a cylindrical region with inner radius of 2 kpc and outer radius of 5 kpc, and we consider again four redshifts between from $z = 1.5$ to $z = 0$, as labeled in the four panels of Figure 14. The average thickness of the galaxies in this radial region shows relatively little evolution with redshift, both in the stellar and the gaseous components. Again we see that the stellar profile substantially grows in amplitude whereas the gas profile shows relatively little evolution. The TEQS model is

ahead in stellar growth at early times, but then TNG catches up so that the models are very similar in stellar mass in this region at late times.

A detailed comparison of the shape of the stellar profile shows that TEQS is slightly more "peaky," i.e., narrower, and the same is true at higher redshift. But these differences are quite small, and in particular, the stellar distributions appear much thicker than naively expected from the thickness of the star-forming gaseous layers in our tall box simulations. This could be at least partially due to the stacking procedure we have applied here. As the cosmologically formed galaxies exhibit warps, corrugations and perturbations such as strong spiral arms, it could be that potentially thin disk structure components are washed out by the averaging procedure. Another possibility is that the disk stars are substantially heated in their vertical structure, for example by perturbations in the disk, by interactions or mergers with satellites, or simply due to numerical noise from two-body relaxation processes related to the *N*-body dynamics. These processes may well be dominant over the intrinsic thickness of the stellar layer initially formed out of the star-forming phase, so that TNG and TEQS produce essentially equally thick galaxies.

## 5. Discussion and Conclusions

In this study we have investigated whether a more modern equation of state model for the treatment of sub-grid star formation, as directly motivated by high-resolution simulations of the star-forming ISM, introduces significant differences compared to the heuristic model that has been used by the IllustrisTNG project. This on one hand serves to test the robustness and validity of the TNG model, and on the other hand has the potential to lead to an improved and ultimately more accurate treatment of star formation in cosmological simulations of galaxy formation.

We have first tested our new TEQS formulation for the equation of state and the star formation law of the ISM on simulations in tall boxes, where the vertical stratification of a star-forming gaseous layer under self-gravity is investigated, which can be viewed as a simple model for a patch excised from a disk galaxy. Our tall box simulations have revealed significant differences in the structural properties and star formation rates between the TEQS and TNG models. The TEQS model tends to create denser and thinner sheets than TNG due to its softer equation of state, which is true at any value of the gas surface density. Because the star formation is also biased toward higher density values in TEQS, the star formation is also more centrally concentrated toward the mid-plane in TEQS, also implying that the formed stellar distributions are in principle expected to have a smaller scale-height than in the TNG model. Note, however, that the total star formation rate surface density is nevertheless not always higher for TEQS. This is only true for high gas surface densities while for values that are close to the star formation threshold the TNG actually has a higher star formation rate surface density, simply because it does not reduce the star formation quite as quickly for a declining density.

We then applied both models to the cosmological formation of Milky Way-sized galaxies, using initial conditions taken from the Auriga simulation project. Because the response of individual systems to changes in the ISM model can be quite different, we simulated a sample of 12 different galaxies in order to be able to average over them and to more clearly identify systematic differences. We have found that the TEQS model consistently produces galaxies with denser cores and smaller overall radial sizes compared to the TNG model. These differences can also be seen in an analyses of the vertical structure, although they disappear at larger heights above the galactic disks. An analysis of the star formation within the galaxy simulations has further corroborated these structural differences. The TEQS model tends to form stars more intensely in the central high-density regions but produces less star formation in the outer exponential disk part of the galaxies. Interestingly, the radial surface density of the gas is very similar in both models, and this quantity also shows only comparatively little radial variation.

When analyzing the vertical structure of the disk galaxies, both in the gas and in the stellar components, we have not been able to identify clear differences in their thickness, which is somewhat unexpected when one takes the tall box results as a guide. This either means that the disk thickness is set by other processes that cause substantial dynamical heating of the stellar disks, thereby overriding the intrinsic thickness of the star-forming gaseous sheet, or it may just appear quite thick due to averaging effects in our stacking analysis, which is not guaranteed to always line-up disk components perfectly. Another possibility would be numerical limitations such as a vertical smoothing due to a comparatively large gravitational softening length. Future work has to clarify which of these explanations is really the correct one. Another important quantity that is essentially invariant when going from TNG to TEQS is the total stellar mass of the galaxies, at least when compared at late times. This suggests that the influences of radiative cooling and feedback processes are ultimately more important for regulating galaxy formation than the equation of state model.

In conclusion, our study highlights the nuanced role that different ISM models play in galaxy formation. By comparing the TEQS and TNG models, we have gained valuable insights into how the changes brought about by TEQS may affect predictions obtained by IllustrisTNG. In particular, it is very interesting to note that despite a fundamentally different star formation law, the predicted galaxy morphology and especially the stellar masses are quite similar. However, there are some notable differences as well, especially in the radial galaxy sizes. This could be quite relevant in comparisons to observations,

and furthermore also influences the rate of bar formation and the pattern speed of bars. It will be interesting for future work to examine the implications of TEQS more broadly, for example in simulations of large periodic volumes, so that its impact on the whole galaxy population can be assessed and used to judge whether TEQS is a more successful effective model than TNG, or whether the high-resolution small-scale simulations need further improvement.

## Acknowledgments

This work is supported by the National SKA Program of China (grant No. 2020SKA0110100), the CAS Project for Young Scientists in Basic Research (No. YSBR-092), the science research grants from the China Manned Space Project with Nos. CMS-CSST-2021-A02 and GHfund C(202407031909). We acknowledge the support by a Max Planck Partner Group led by Hong Guo at SHAO and the use of the High Performance Computing Resource in the Core Facility for Advanced Research Computing at the Shanghai Astronomical Observatory.

## ORCID iDs

Yiheng Wu https://orcid.org/0009-0004-6083-6608
Volker Springel https://orcid.org/0000-0001-5976-4599

## References

Conselice, C. J. 2014, ARA&A, 52, 291
Crain, R. A., Schaye, J., Bower, R. G., et al. 2015, MNRAS, 450, 1937
Furlong, M., Bower, R. G., Crain, R. A., et al. 2017, MNRAS, 465, 722
Genel, S., Vogelsberger, M., Springel, V., et al. 2014, MNRAS, 445, 175
Girichidis, P., Walch, S., Naab, T., et al. 2016, MNRAS, 456, 3432
Grand, R.J.J., Gómez, F.A., Marinacci, F., et al. 2017, MNRAS, 467, 179
Guedes, J., Callegari, S., Madau, P., & Mayer, L. 2011, ApJ, 742, 76
Hopkins, P. F., Kereš, D., Oñorbe, J., et al. 2014, MNRAS, 445, 581
Kennicutt, R.C.J. 1989, ApJ, 344, 685
Kennicutt, R.C.J. 1998, ApJ, 498, 541
Kim, C.-G., & Ostriker, E. C. 2017, ApJ, 846, 133
Kim, C.-G., Ostriker, E. C., & Kim, W.-T. 2013, ApJ, 776, 1
Moore, B., Katz, N., Lake, G., Dressler, A., & Oemler, A. 1996, Natur, 379, 613
Naab, T., & Ostriker, J. P. 2017, ARA&A, 55, 59
Nelson, D., Pillepich, A., Springel, V., et al. 2018, MNRAS, 475, 624
Ostriker, E. C., & Kim, C.-G. 2022, ApJ, 936, 137
Ostriker, E. C., & Shetty, R. 2011, ApJ, 731, 41
Pillepich, A., Nelson, D., Hernquist, L., et al. 2018a, MNRAS, 475, 648
Pillepich, A., Springel, V., Nelson, D., et al. 2018b, MNRAS, 473, 4077
Robertson, B., Yoshida, N., Springel, V., & Hernquist, L. 2004, ApJ, 606, 32
Shen, S., Mo, H. J., White, S. D. M., et al. 2003, MNRAS, 343, 978
Springel, V. 2010, MNRAS, 401, 791
Springel, V., Di Matteo, T., & Hernquist, L. 2005, MNRAS, 361, 776
Springel, V., & Hernquist, L. 2003, MNRAS, 339, 289
Vogelsberger, M., Genel, S., Springel, V., et al. 2014a, MNRAS, 444, 1518
Vogelsberger, M., Genel, S., Springel, V., et al. 2014b, Natur, 509, 177
Walch, S., Girichidis, P., Naab, T., et al. 2015, MNRAS, 454, 238
Weinberger, R., Springel, V., & Pakmor, R. 2020, ApJS, 248, 32
Weinberger, R., Springel, V., Hernquist, L., et al. 2017, MNRAS, 465, 3291